Supporting Information

Hypercoordinated Si/Ge Driving Excellent HER Catalytic Performance in New TM$_2$X (X = Si and Ge) Monolayers: A High-Throughput Investigation by Screening Transition Metal Elements

Tianya Li[a], Guangtao Yu[a,*], E Yang[a], Wei Chen[a,b,c,*]

[a]Engineering Research Center of Industrial Biocatalysis, Fujian Provincial Key Laboratory of Advanced Materials Oriented Chemical Engineering, Fujian-Taiwan Science and Technology Cooperation Base of Biomedical Materials and Tissue Engineering, College of Chemistry and Materials Science, Fujian Normal University, Fuzhou, 350007, China
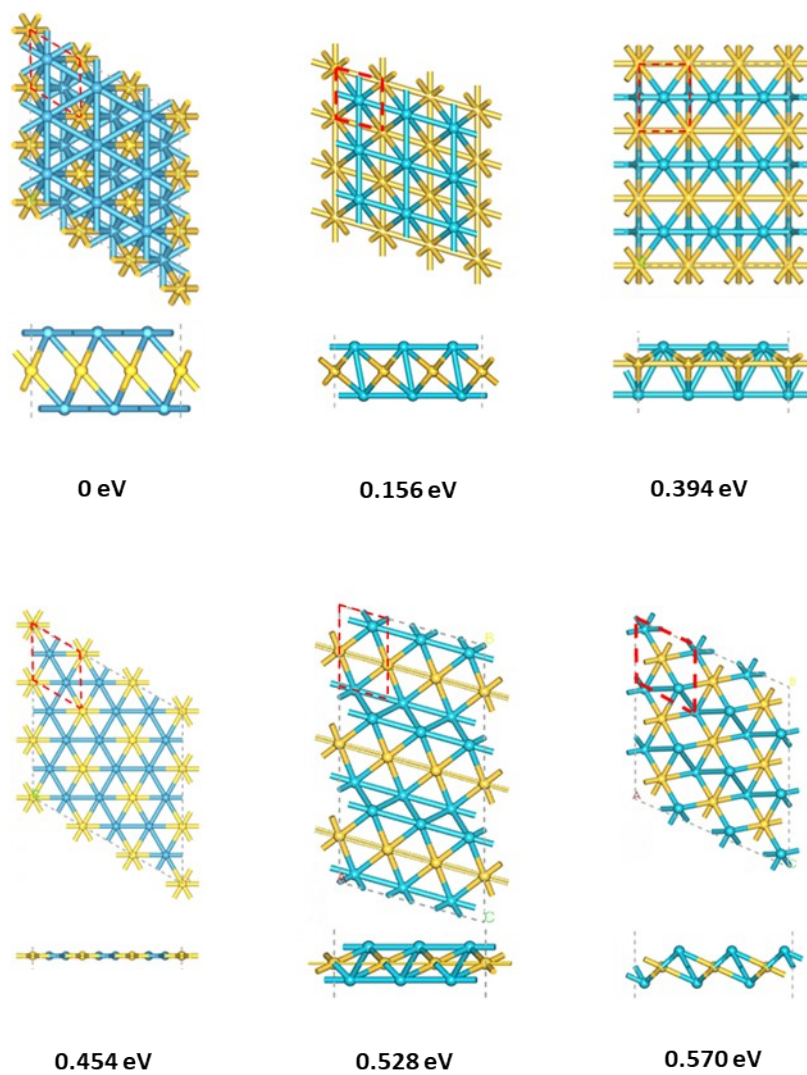
[b]Academy of Carbon Neutrality of Fujian Normal University, Fuzhou, 350007, China

[c]Fujian Provincial Key Laboratory of Theoretical and Computational Chemistry, Xiamen University, Xiamen, 361005, China
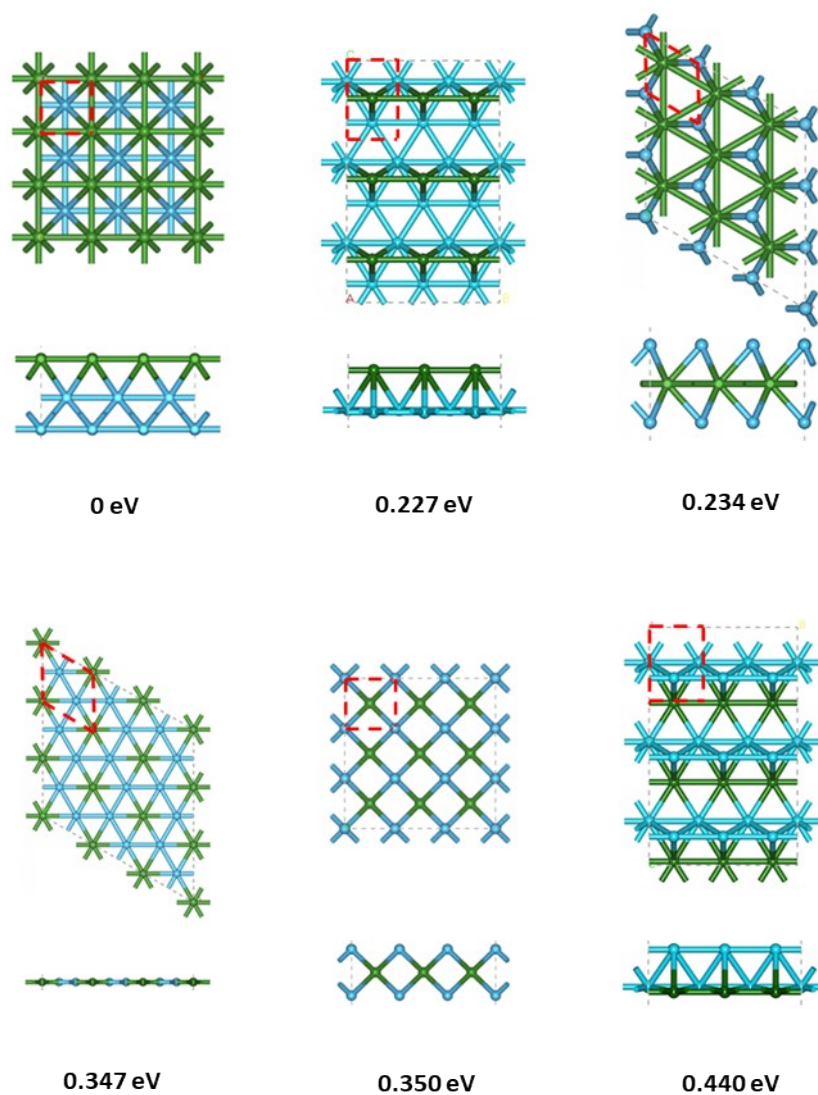
*Corresponding author.

E-mail: yugt@fjnu.edu.cn (Guangtao Yu), chenwei@fjnu.edu.cn (Wei Chen)

1. Supporting Figures

Figure S1. Possible 2D Co_2Si structures obtained through the PSO simulation implemented in CALYPSO code. The relative energy per atom is indicated.

0 eV
0.227 eV
0.234 eV

0.347 eV
0.350 eV
0.440 eV

Figure S2. Possible 2D Co_2Ge structures obtained through the PSO simulation implemented in CALYPSO code. The relative energy per atom is indicated.
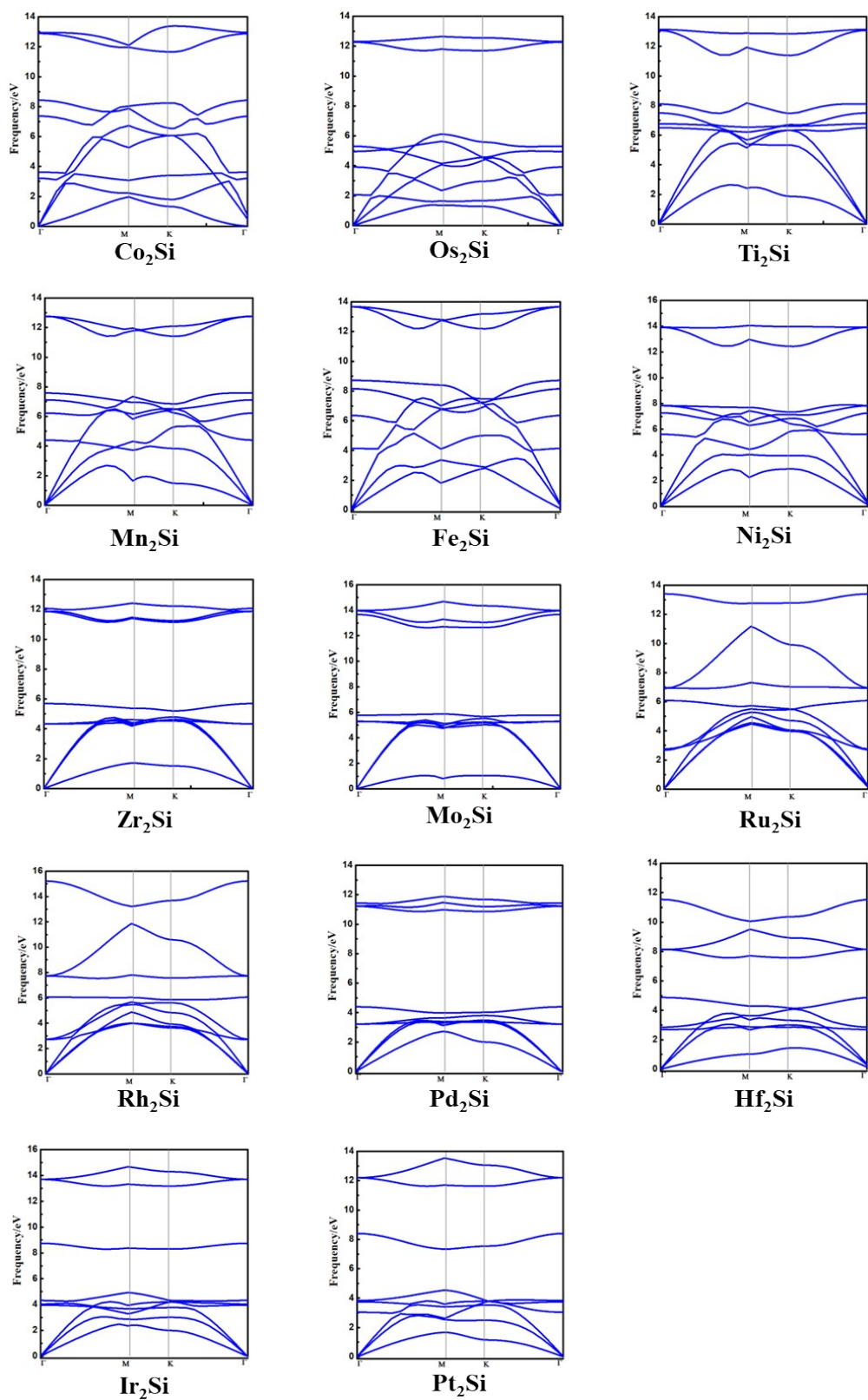
Figure S3. Phonon spectrum of the TM$_2$Si series.

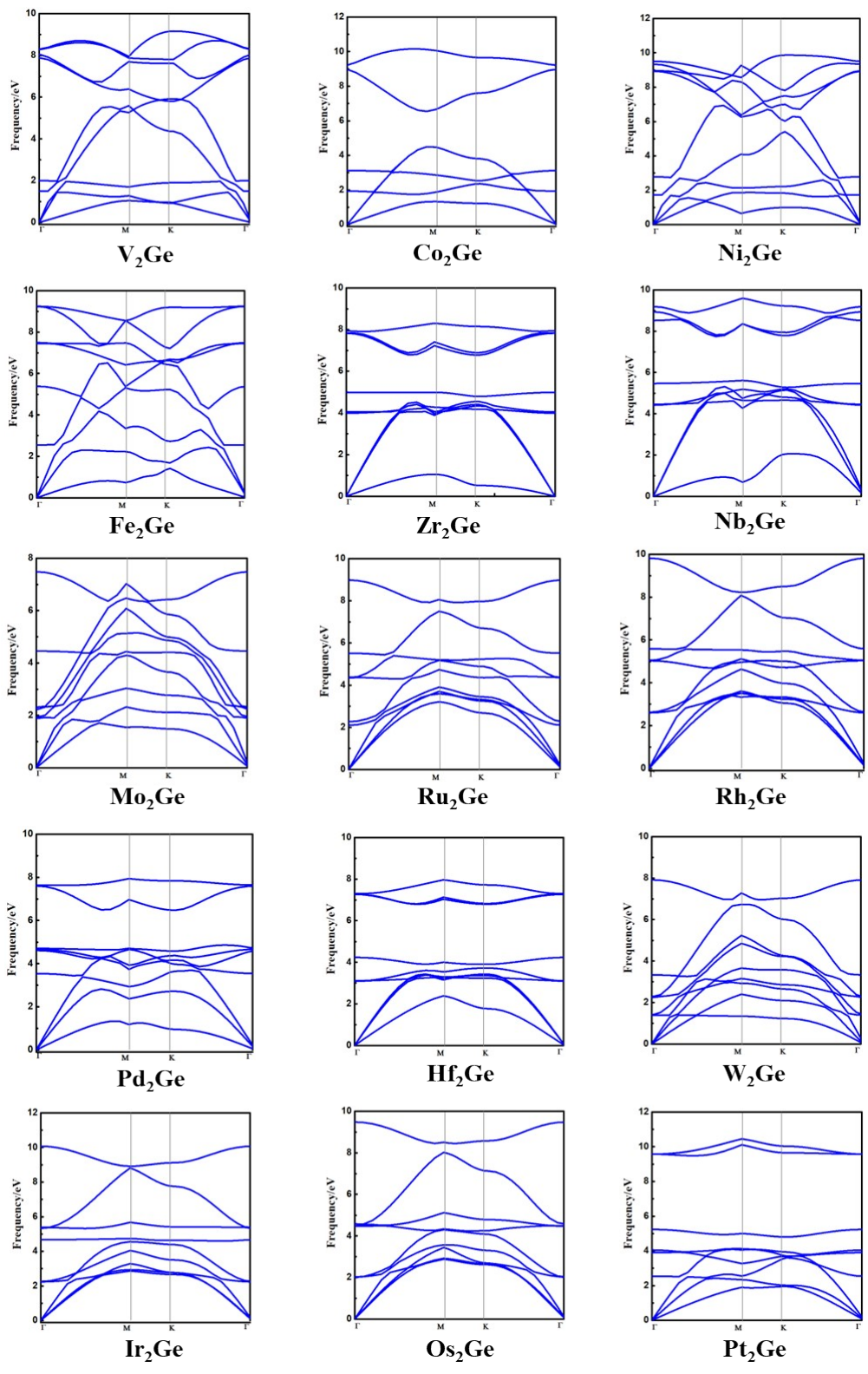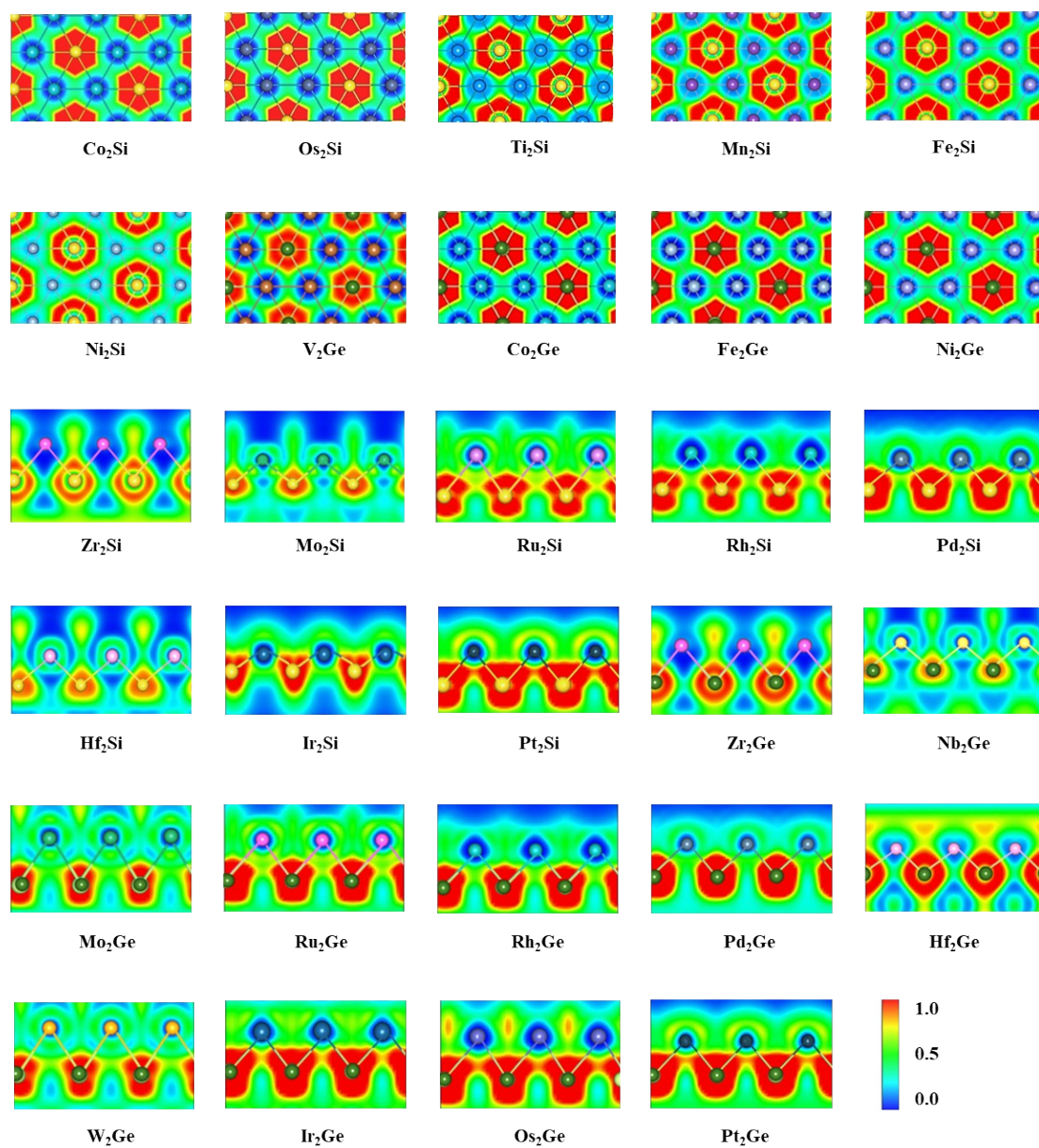**Figure S4.** Phonon spectrum of the TM$_2$Ge series.

Figure S5. ELF maps of the TM$_2$X (X=Si and Ge) systems, where the pictures in the first two rows are the top views of the planar and quasi-planar monolayers, and the others are the side views of the buckled monolayers.
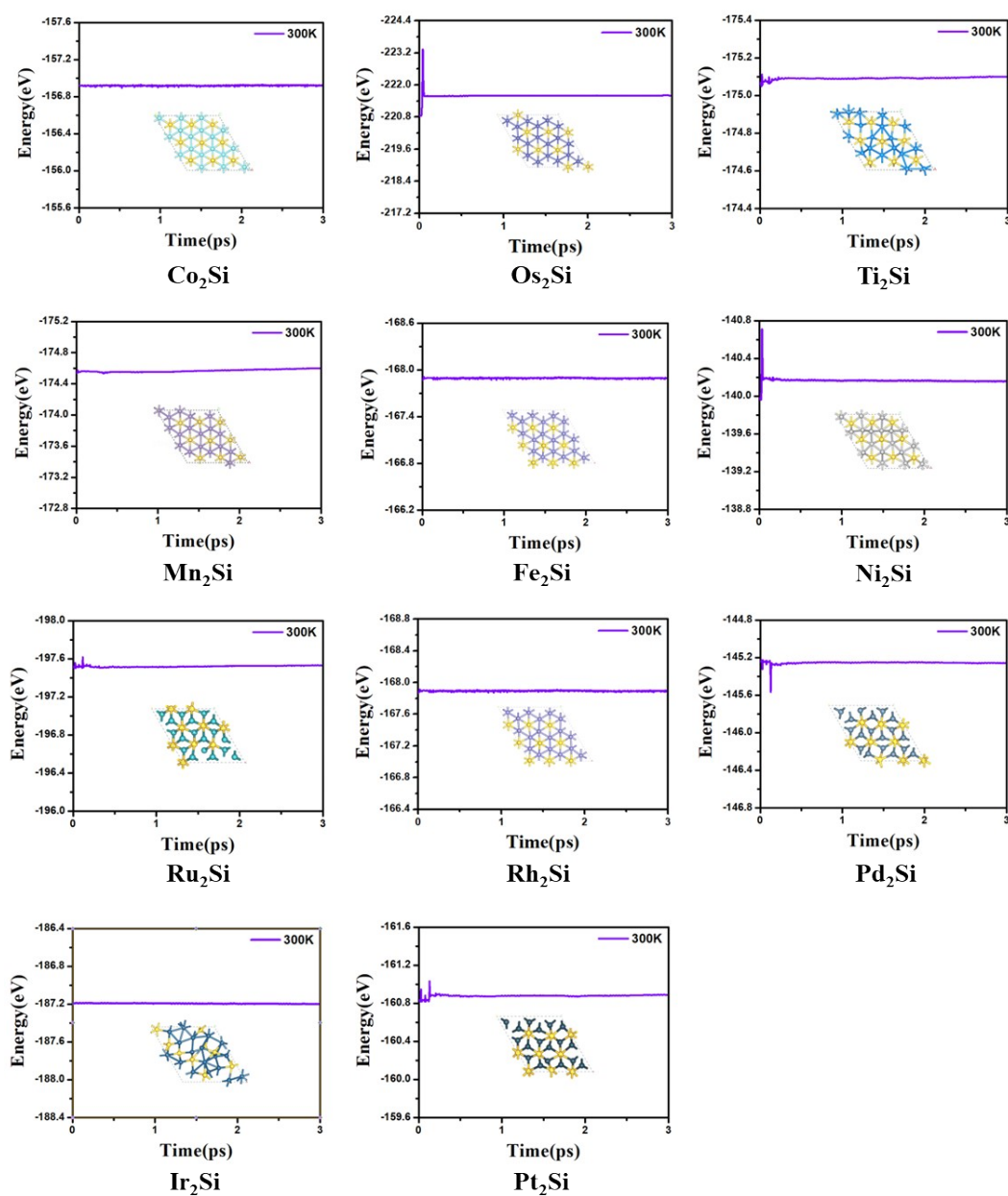
Figure S6. Evolution of total energy of the TM$_2$Si monolayers at 300 K from AIMD, and the corresponding snapshots after 3 *ps*.
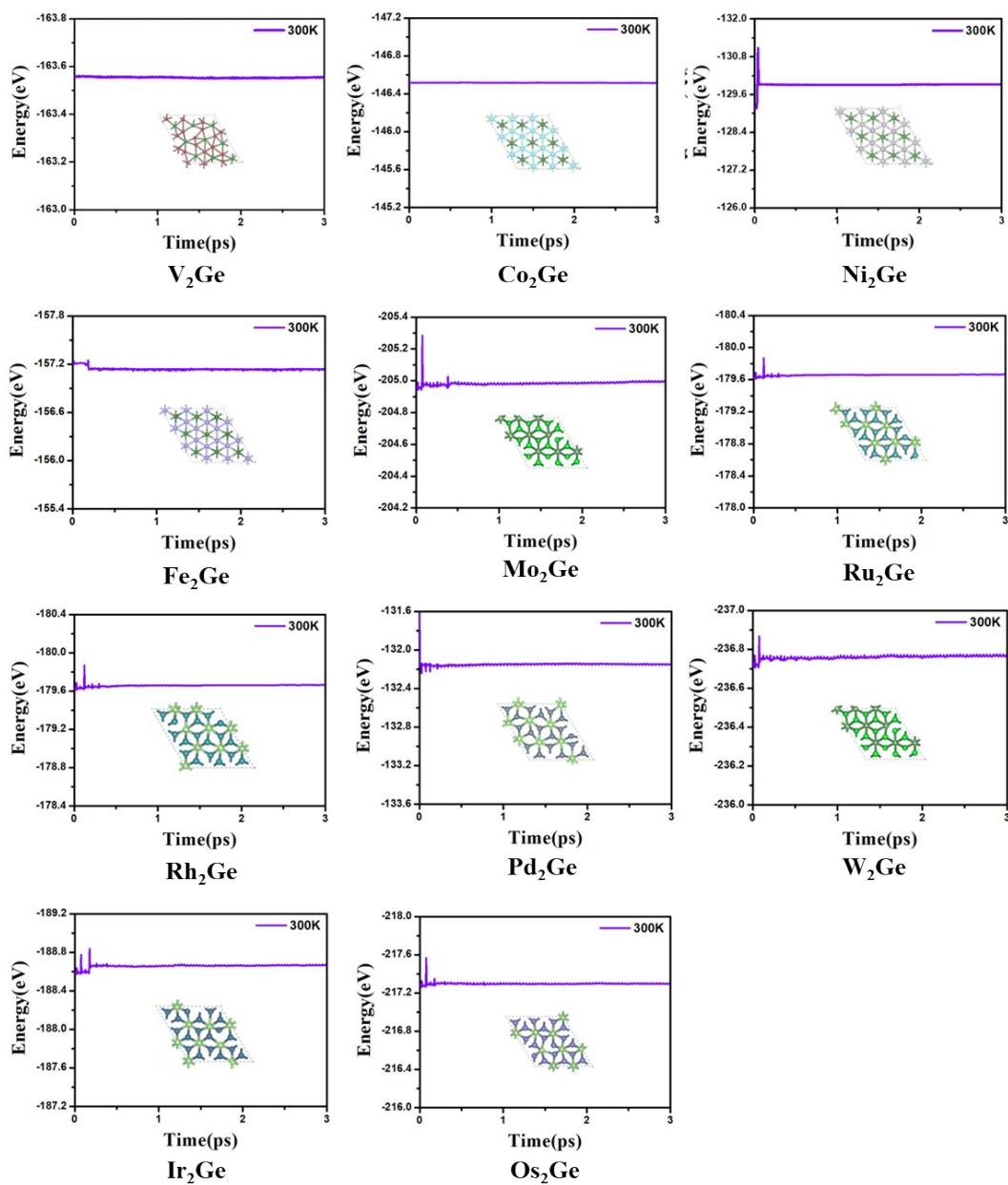
Figure S7. Evolution of total energy of the TM$_2$Ge monolayers at 300 K from AIMD, and the corresponding snapshots after 3 *ps*.
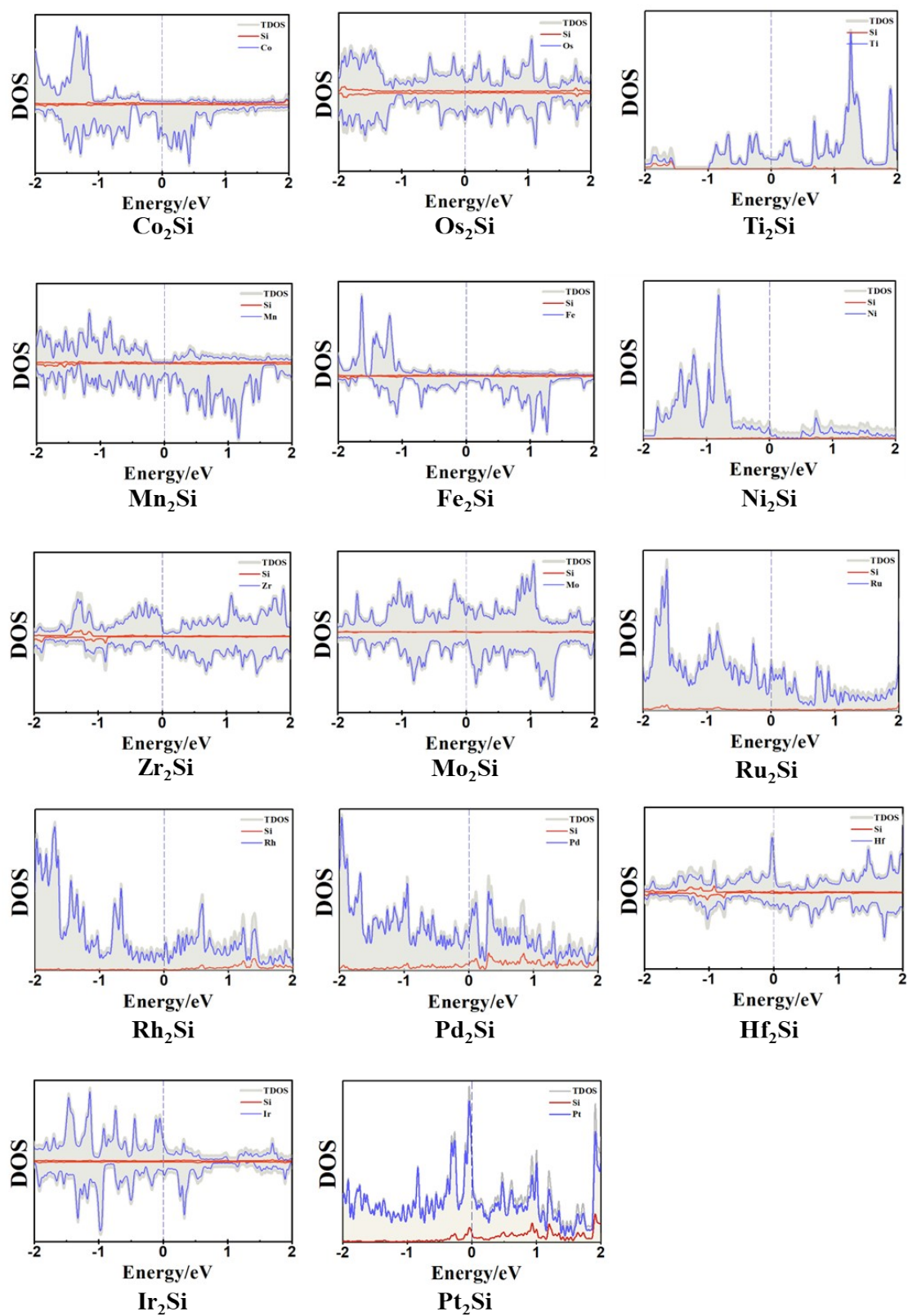
Figure S8. The calculated DOSs of the TM$_2$Si systems.
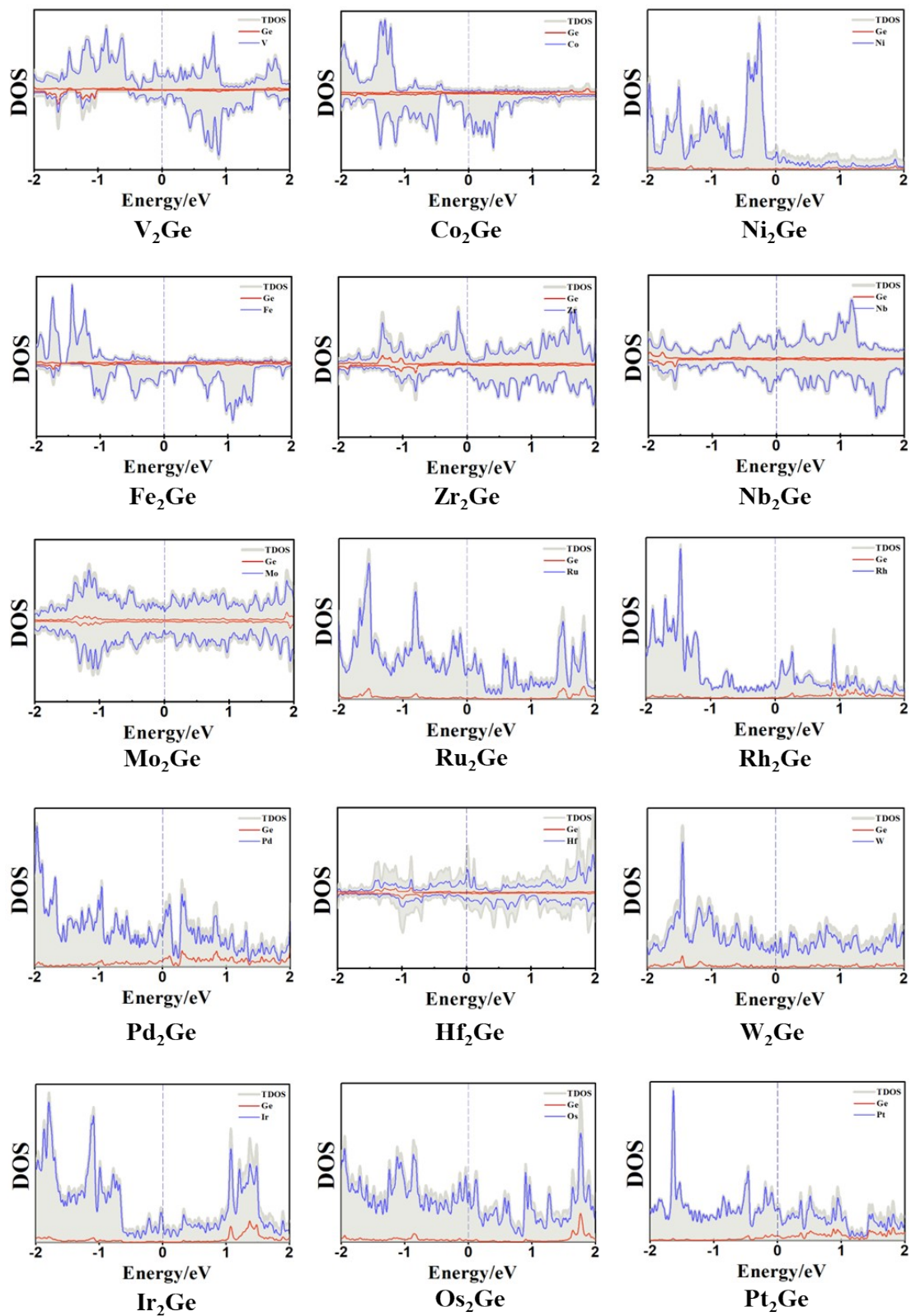
Figure S9. The calculated DOSs of the TM$_2$Ge systems.
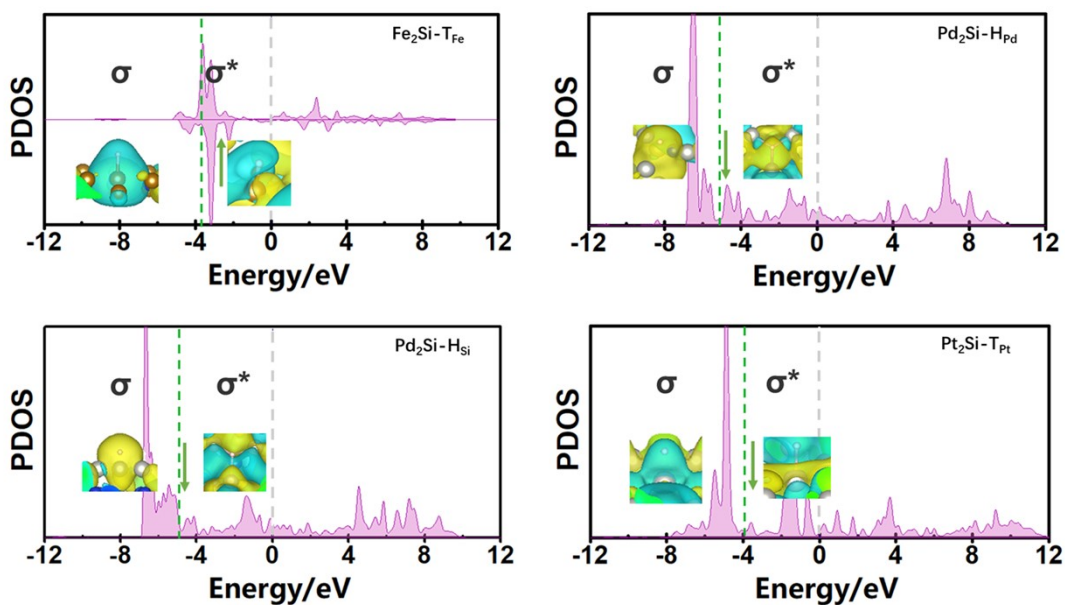
Figure S10. Partial density of states (PDOS) about the 1s orbital of H atom after the H adsorption of TM_2Si (TM=Fe, Pd and Pt). The Fermi level is set to zero marked by the gray dashed line. Inset: molecular orbitals related to the H atom adsorbed at the active site in different energy ranges marked by the green dashed line. The green arrow represents the σ_{1S}-center of the adsorbed H.
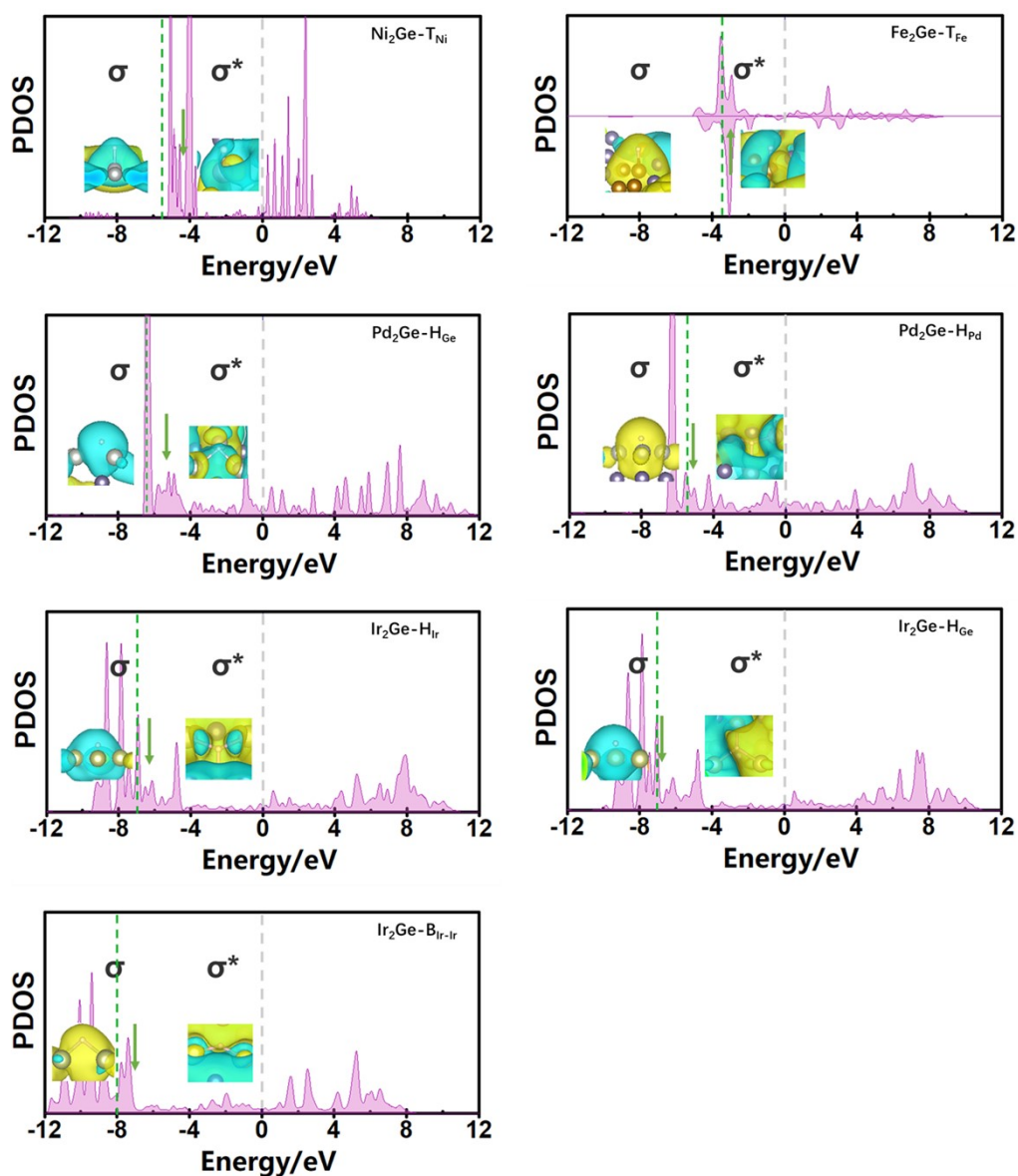
Figure S11. Partial density of states (PDOS) about the 1s orbital of H atom after the H adsorption of TM_2Ge (TM= Ni, Fe, Pd and Ir). The Fermi level is set to zero marked by the gray dashed line. Inset: molecular orbitals related to the H atom adsorbed at the active site in different energy ranges marked by the green dashed line. The green arrow represents the σ_{1S}-center of the adsorbed H.
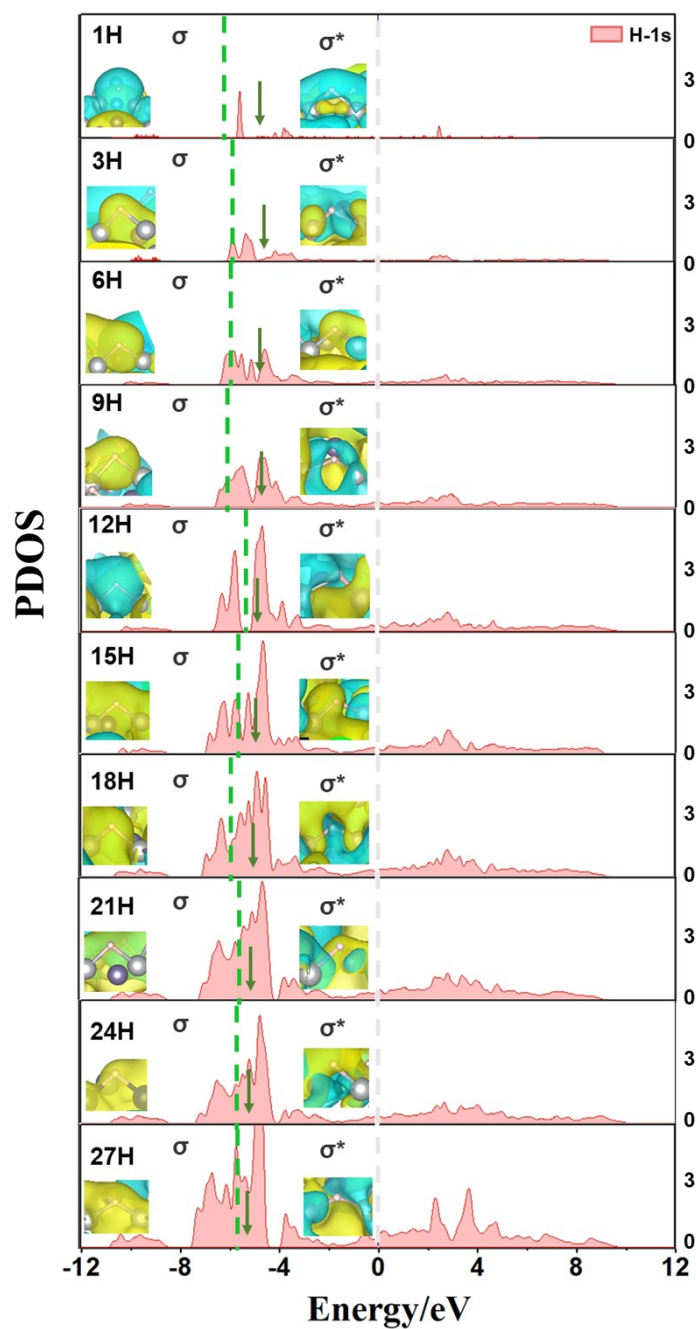
Figure S12. PDOS about the 1s orbitals of H atoms as well as the σ_{1S}-center for H adsorbed on the Ni_2Ge monolayer under the different H coverages. The Fermi level is set to zero marked by the gray dashed line. Inset: Molecular orbitals related to the H atom adsorbed at the active site in different energy ranges marked by the green dashed line. The green arrow represents the σ_{1S}-center of the adsorbed H.
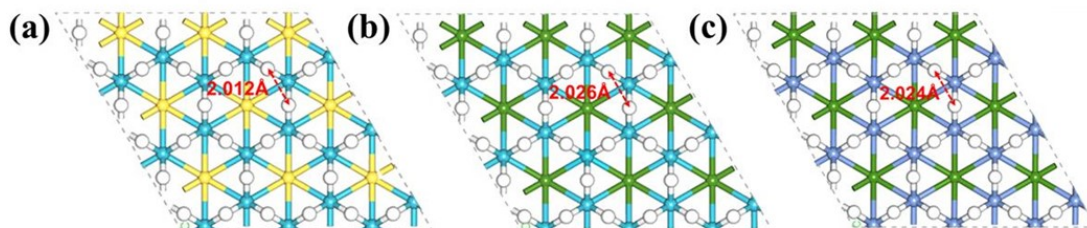
Figure S13. The calculated distance between two adjacent H atoms on the 2D Co_2Si (a), Co_2Ge (b), and Ni_2Ge (c) monolayers at the highest hydrogen coverage (θ_{H*} = 3 ML).

2. Supporting Tables

Table S1. The solvent effect on the computed ΔG_{H*} values of the sampled Co_2Si monolayer.

Adsorption sites	ΔG_{H*} (eV) without solvation	ΔG_{H*} (eV) with solvation
B_{Co-Co}	-0.076	-0.077
T_{Co}	0.101	0.110
T_{Si}	0.346	0.357

Table S2. The calculated ΔG_{H*} values of 2D Co_2Si and Co_2Ge monolayers under the DFT+U method.

Adsorption sites	Co₂Si		Co₂Ge	
	ΔG_{H*} (eV) without U_{eff}	ΔG_{H*} (eV) with U_{eff}	ΔG_{H*} (eV) without U_{eff}	ΔG_{H*} (eV) with U_{eff}
B_{Co-Co}	-0.076	-0.120	-0.083	-0.099
T_{Co}	0.101	0.052	0.095	0.074
$T_{Si/Ge}$	0.346	0.329	0.604	0.574

Table S3. Structural information of the predicted TM$_2$Si monolayers, including the lattice parameters (a and b), bond lengths, and buckled heights (h).

Systems		a=b (Å)	Bond Lengths (Å)		h (Å)
			TM-TM	TM-Si	
Planar	Co$_2$Si	4.005	2.309	2.309	0
	Os$_2$Si	3.486	2.460	2.460	0
Quasi-planar	Ti$_2$Si	3.933	2.925	2.451	1.842
	Mn$_2$Si	3.890	2.668	2.358	1.440
	Fe$_2$Si	3.931	2.418	2.308	0.831
	Ni$_2$Si	3.780	2.526	2.215	1.404
Buckled	Zr$_2$Si	3.600	(3.681)	2.574	3.038
	Mo$_2$Si	3.409	(3.253)	2.356	2.590
	Ru$_2$Si	2.715	(3.976)	2.407	3.654
	Rh$_2$Si	2.800	(3.819)	2.368	3.460
	Pd$_2$Si	3.190	(3.553)	2.387	3.038
	Hf$_2$Si	3.600	(3.692)	2.578	3.050
	Ir$_2$Si	3.560	(2.970)	2.318	2.144
	Pt$_2$Si	2.985	(3.722)	2.385	3.299

Table S4. Structural information of the predicted TM$_2$Ge monolayers, including the lattice parameters (a and b), bond lengths, and buckled heights (h).

Systems		a=b (Å)	Bond Lengths (Å)		h (Å)
			TM-TM	TM-Si	
Planar	V$_2$Ge	4.450	2.569	2.569	0
	Co$_2$Ge	4.078	2.355	2.355	0
	Ni$_2$Ge	4.105	2.349	2.349	0
Quasi-planar	Fe$_2$Ge	4.051	2.456	2.369	0.750
Buckled	Zr$_2$Ge	3.630	(3.771)	2.610	3.134
	Nb$_2$Ge	3.490	(3.557)	2.492	2.931
	Mo$_2$Ge	2.750	(4.662)	2.706	4.383
	Ru$_2$Ge	2.770	(4.154)	2.496	3.834
	Rh$_2$Ge	2.880	(3.951)	2.450	3.584
	Pd$_2$Ge	3.143	(3.816)	2.472	3.356
	Hf$_2$Ge	3.602	(3.773)	2.607	3.148
	W$_2$Ge	2.750	(4.646)	2.695	4.356
	Os$_2$Ge	2.754	(4.189)	2.507	3.876
	Ir$_2$Ge	2.835	(3.999)	2.451	3.649
	Pt$_2$Ge	3.050	(3.863)	2.461	3.438

Table S5. The TM-TM and TM-Si bond lengths in TM_2Si, as well as in the relevant material systems synthesized experimentally.

Systems		Bond Lengths (Å)					
		TM-TM			TM-Si		
		In this study	In relevant experimental materials		In this study	In relevant experimental materials	
Planar	Co_2Si	2.309	2.470	Co	2.309	2.488	Co_3Si
	Os_2Si	2.460	2.682	Os	2.460	2.554	OsSi
Quasi-planar	Ti_2Si	2.925	2.936	Ti	2.451	2.547	$TiSi_2$
	Mn_2Si	2.668	2.750	Mn	2.358	2.529	Mn_3SiIr
	Fe_2Si	2.418	2.585	Fe	2.308	2.766	$Fe_{11}Si_5$
	Ni_2Si	2.526	2.630	TiNi(TiCo)	2.215	2.332	$NiSi_2$
Buckled	Zr_2Si	--	--	--	2.574	2.778	ZrFeSi
	Mo_2Si	--	--	--	2.356	2.605	$MoSi_2$
	Ru_2Si	--	--	--	2.407	2.412	RuSi
	Rh_2Si	--	--	--	2.368	2.483	RhSi
	Pd_2Si	--	--	--	2.387	2.488	HfSiPd
	Hf_2Si	--	--	--	2.578	2.750	HfSiPd
	Ir_2Si	--	--	--	2.318	2.393	Mn_3SiIr
	Pt_2Si	--	--	--	2.385	2.421	Pt_2Si_3

Table S6. The TM-TM and TM-Ge bond lengths in TM$_2$Ge, as well as in the relevant material systems synthesized experimentally.

Systems		Bond Lengths (Å)					
		TM-TM			TM-Ge		
		In this study	In relevant experimental materials		In this study	In relevant experimental materials	
Planar	V$_2$Ge	2.569	2.583	V	2.569	2.650	V$_3$Ge
	Co$_2$Ge	2.355	2.470	Co	2.355	2.372	Co$_5$Ge$_7$
	Ni$_2$Ge	2.349	2.496	Ni$_3$Ge	2.349	2.496	Ni$_3$Ge
Quasi-planar	Fe$_2$Ge	2.456	2.482	Fe$_{13}$Ge$_3$	2.369	2.511	Fe$_{13}$Ge$_3$
Buckled	Zr$_2$Ge	--	--	--	2.610	2.861	ZrGeIr
	Nb$_2$Ge	--	--	--	2.492	2.910	Nb$_3$Ge
	Mo$_2$Ge	--	--	--	2.706	2.710	Mo$_3$Ge
	Ru$_2$Ge	--	--	--	2.496	2.444	ScRuGe$_2$
	Rh$_2$Ge	--	--	--	2.450	2.468	RhGe
	Pd$_2$Ge	--	--	--	2.472	2.453	TiPdGe
	Hf$_2$Ge	--	--	--	2.607	2.755	HfGe$_2$
	W$_2$Ge	--	--	--	2.695	2.700	WGe$_2$
	Os$_2$Ge	--	--	--	2.507	2.510	OsGe$_2$
	Ir$_2$Ge	--	--	--	2.451	2.502	ZrIrGe
	Pt$_2$Ge	--	--	--	2.461	2.462	PtGeS

Table S7. The calculated elastic coefficients of the TM$_2$Si monolayers.

Systems	$C_{11}=C_{22}$	C_{12}	C_{66}
Ti$_2$Si	135.588	114.969	10.314
Mn$_2$Si	248.812	64.710	92.051
Fe$_2$Si	489.270	207.126	140.653
Co$_2$Si	134.790	54.386	40.176
Ni$_2$Si	281.647	5.152	138.247
Zr$_2$Si	372.698	168.653	102.022
Mo$_2$Si	473.650	71.769	200.941
Ru$_2$Si	1296.801	477.474	409.663
Pd$_2$Si	106.312	15.037	45.637
Hf$_2$Si	607.575	190.661	208.456
Ir$_2$Si	472.927	261.131	105.898
Pt$_2$Si	254.809	31.293	111.758

Table S8. The calculated elastic coefficients of the TM$_2$Ge monolayers.

Systems	C$_{11}$=C$_{22}$	C$_{12}$	C$_{66}$
V$_2$Ge	449.825	173.187	138.319
Fe$_2$Ge	363.835	198.101	82.867
Co$_2$Ge	110.082	43.175	32.537
Ni$_2$Ge	476.347	341.836	67.256
Zr$_2$Ge	258.205	147.002	55.602
Nb$_2$Ge	353.544	192.171	80.686
Ru$_2$Ge	1220.584	365.860	427.362
Rh$_2$Ge	602.608	169.360	216.624
Hf$_2$Ge	610.430	181.581	224.425
Os$_2$Ge	1462.744	835.523	313.610
Ir$_2$Ge	1203.100	321.130	440.985
Pt$_2$Ge	63.245	42.958	10.644

Table S9. The computed ΔG_{H^*} values for TM$_2$Si systems. The symbol "--" indicates that structures with adsorbed H* cannot be obtained.

Systems	Adsorption sites	ΔG_{H^*} (eV)
Ti$_2$Si	--	
Mn$_2$Si	--	
Fe$_2$Si	T$_{Fe1}$	0.242
Co$_2$Si	T$_{Si}$	0.346
	T$_{Co}$	0.101
	B$_{Co-Co}$	-0.076
Ni$_2$Si	--	
Zr$_2$Si	H$_{Zr}$	-1.068
	H$_{Si}$	-1.018
Mo$_2$Si	--	
Ru$_2$Si	H$_{Ru}$	-0.415
	T$_{Ru}$	-0.390
Rh$_2$Si	--	
Pd$_2$Si	H$_{Pd}$	0.076
	H$_{Si}$	0.246
Hf$_2$Si	H$_{Hf}$	-0.847
	H$_{Si}$	-1.094
Os$_2$Si	T$_{Si}$	-0.780
	T$_{Os}$	-1.351
Ir$_2$Si	--	
Pt$_2$Si	T$_{Pt}$	0.203
	H$_{Pt}$	0.328
	B$_{Pt--Pt}$	0.292

Table S10. The computed ΔG_{H*} values for TM$_2$Ge systems. The symbol "--" indicates that structures with adsorbed H* cannot be obtained.

Systems	Adsorption sites	ΔG_{H*} (eV)
V$_2$Ge	B$_{V\text{-}V}$	-0.504
Fe$_2$Ge	T$_{Fe1}$	0.175
	T$_{Fe2}$	-0.197
	B$_{Fe\text{-}Fe}$	-0.293
Co$_2$Ge	T$_{Ge}$	0.604
	T$_{Co}$	0.095
	B$_{Co\text{-}Co}$	-0.083
Ni$_2$Ge	T$_{Ge}$	0.551
	T$_{Ni}$	0.207
	B$_{Ni\text{-}Ni}$	-0.333
Zr$_2$Ge	H$_{Zr}$	-1.362
	H$_{Ge}$	-1.346
Nb$_2$Ge	--	
Mo$_2$Ge	H$_{Mo}$	-1.129
	H$_{Ge}$	-1.644
Ru$_2$Ge	H$_{Ru}$	0.881
	T$_{Ru}$	-0.468
Rh$_2$Ge	T$_{Rh}$	-0.984
	H$_{Rh}$	-1.498
	H$_{Ge}$	-1.369
Pd$_2$Ge	H$_{Pd}$	0.002
	H$_{Ge}$	0.120
Hf$_2$Ge	H$_{Hf}$	-1.309
	H$_{Ge}$	-1.572
W$_2$Ge	T$_W$	-1.183
	H$_W$	-0.693
	H$_{Ge}$	-0.726
Os$_2$Ge	H$_{Os}$	-0.754
Ir$_2$Ge	T$_{Ir}$	0.351
	H$_{Ir}$	0.152
	H$_{Ge}$	0.212
	B$_{Ir\text{--}Ir}$	0.218
Pt$_2$Ge	--	

Table S11. The σ_{1S} centers for H adsorption on TM$_2$Si (TM=Co, Fe, Pd and Pt) monolayers.

Systems	Adsorption sites	σ_{1S} centers (eV)
Co$_2$Si	T$_{Co}$	-4.026
	B$_{Co\text{-}Co}$	-4.855
Fe$_2$Si	T$_{Fe1}$	-3.255
Pd$_2$Si	H$_{Pd}$	-4.888
	H$_{Si}$	-4.870
Pt$_2$Si	T$_{Pt}$	-3.816

Table S12. The σ_{1S} centers for H adsorption on TM$_2$Ge (TM=Co, Ni, Fe, Pd and Ir) monolayers.

Systems	Adsorption sites	σ_{1S} centers (eV)
Co$_2$Ge	T$_{Co}$	-3.994
	B$_{Co-Co}$	-4.778
Ni$_2$Ge	T$_{Ni}$	-4.323
Fe$_2$Ge	T$_{Fe1}$	-3.192
Pd$_2$Ge	H$_{Pd}$	-5.104
	H$_{Ge}$	-5.116
Ir$_2$Ge	H$_{Ir}$	-6.285
	H$_{Ge}$	-6.918
	B$_{Ir--Ir}$	-7.005

Table S13. The σ_{1S} centers for H adsorption on the Co_2Si, Co_2Ge and Ni_2Ge monolayers under the different H coverage.

n	σ_{1S} centers (eV)		
	Co_2Si	Co_2Ge	Ni_2Ge
1	-4.855	-4.778	-4.840
3	-4.708	-4.774	-4.745
6	-4.881	-4.679	-4.918
9	-5.062	-4.669	-4.866
12	-4.984	-4.820	-4.910
15	-4.959	-4.770	-5.066
18	-4.935	-4.788	-5.107
21	-5.062	-4.916	-5.210
24	-5.281	-5.073	-5.268
27	-5.407	-5.167	-5.475